J Mol Model (2009) 15:1229–1236
DOI 10.1007/s00894-009-0474-5

ORIGINAL PAPER

A butterfly effect: highly insecticidal resistance caused by only a conservative residue mutated of drosophila melanogaster acetylcholinesterase

Feng Fan · Zhiqi You · Zhong Li · Jiagao Cheng · Yun Tang · Zhenhua Tang

Received: 15 December 2008 / Accepted: 26 January 2009 / Published online: 5 March 2009

Abstract Acetylcholinesterase (AChE) and its mutation recently emerged as a significant research area, due to its resistance against organophosphate and carbamate insecticides. Residue G265, which is always a conservative residue, mutated to A265 is the most frequent mutant of AChE in Drosophila populations. However, only this mutation caused a 'butterfly effect' that gives high insecticidal resistance. Herein, the models of sensitive strain (Dm-S) and the resistance strain (Dm-R) were constructed, to give a total of 2000 ps molecular dynamics simulation and to reveal the insecticidal resistance mechanism, with implied, the active gorge of Dm-R was much less flexible than that of Dm-S. The "back door" channel was widened to accelerate the detoxication against insecticides by the conformation changing of W83 and I161. All the distances (S238-H480, S238-G150, S238-G151, Y71-M153) in Dm-R became smaller than those in Dm-S, which may deeply influence the binding between the insecticides and DmAChE.

Keywords Covalent docking · DmAChE · Insecticidal resistance · Molecular dynamics

F. Fan · Z. You · Z. Li (✉) · J. Cheng · Z. Tang
Shanghai Key Lab of Chemical Biology,
East China University of Science and Technology,
P.O. Box 544, 130 Meilong Road,
Shanghai 200237, China
e-mail: lizhong@ecust.edu.cn

F. Fan · Z. You · Z. Li · J. Cheng · Y. Tang · Z. Tang
School of Pharmacy,
East China University of Science and Technology,
130 Meilong Road,
Shanghai 200237, China

Introduction

Acetylcholinesterase (AChE, EC 3.1.1.7) regulates the level of acetylcholine and terminates nerve impulses by catalyzing the hydrolysis of acetylcholine. As AChE's irreversible inhibitors, organophosphate (OP) and carbamate (CA) insecticides leads to an accumulation of acetylcholine in the synapses which in turn leaves the acetylcholine receptors permanently open, resulting in the death of the insect [1–3]. However, since the 1940s, the frequent and excess usage of these insecticides have developed resistance. To date, three main mechanisms of resistance have been reported: reduction of insecticide penetration, increasing degradation of insecticides, and most important, the modification of the insecticide targets, to which AChE belongs [4].

Up to now, many studies [5–9] have revealed the relationship between insecticidal resistance and the alerted AChE. And the mutations of residues in AChE may provide insecticidal resistance [10–14]. By means of genetic engineering, the "Ace" locus that encodes AChE has been identified [15]. In some insects, two kinds of locus named "Ace-1" and "Ace-2" were found. Mutation in Ace-1 contributes to high insecticidal resistance [16–19].

By now, the most effective approach to resolve the resistance problem is to find negative cross-insensitivity compounds. In fact, some mutational AChEs have indicated a negative cross-insensitivity against a variety of OP and CA inhibitors [20, 21], as earlier suggested by Brown [22]. It might be a possible stratagem to find novel inhibitors based on negatively correlated insecticides in resistance management programs.

Drosophila melanogaster acetylcholinesterase (DmAChE) is a typical target in insect. It has an active gorge about 20 Å depth from the peripheral anionic site (PAS) to the catalytic

triad. There are seven active sites in the active gorge: catalytic triad, choline binding site, acyl pocket, oxyanion hole, PAS, aromatic guidance region and backdoor opening region [23] (See Fig. 1). OPs and CAs can act as "hemisubstrates" to trap the enzyme *via* forming a covalent bond with the serine 238. Even that some OP-AChE conjugates undergo post-inhibitory reactions, collectively called "aging", which result in truly irreversible enzyme inhibition [24]. However, around the active valley, mutations of I161 V, G265A, F330Y and G368A give insecticidal resistance. Each mutational DmAChE gets the different insecticidal resistance [4]. The insecticidal resistance mechanism of mutational DmAChE is very complicated and not clear yet.

Molecular dynamics (MD) simulation is a powerful tool to analyze the structural and dynamic features of biomacromolecules. It provides information about atomic interaction and their time evolution at a level of detail which can both enhance and complement the experimental results [25–28]. The MD simulation will focus on the apo-proteins without ligands. The MD simulation results will be combined with the ligands for further quantum mechanics/molecular mechanics (QM/MM) research. Also the MD simulation results may be useful for virtual screening of negative cross-insensitivity compounds discovery for further work.

The single point mutation, the glycine 265 mutating to alanine of DmAChE, is the most frequent mutation in Drosophila populations [2]. So in our work, the mutational amino acid residue G265A is raised for computer aided research. MD simulation is applied to expose the insecticidal resistance mechanism of mutational DmAChE. MD simulation and docking technology can be combined in drug design, where the flexibility of protein is considered [29].

Materials and methods

Protein preparation

DmAChE crystal structure was obtained from the Protein Data Bank (PDB), entry code 1QO9. The lost loop region 104–135 was re-modeled by loop search method (including energy minimized optimization) in Sybyl7.0 (molecular modeling software package, Tripos Associates, Inc., St. Louis), which resulted in the wild type DmAChE, i.e., sensitive strain model (Dm-S). After making the mutation of G265A, the DmAChE resistant strain model (Dm-R) was constructed.

Molecular dynamics simulations

The MD simulations were performed on a DELL PowerEdge cluster, using program CHARMM [30] (version c31b1) and the all-atom version 22 force field [31, 32]. The TIP3P water model was used to simulate the solvent [33].

Dm-S and Dm-R were simulated separately under the same conditions. The starting coordinates of each protein came from the prepared structural model. All hydrogen atoms were then added by CHARMM subroutine HBUILD

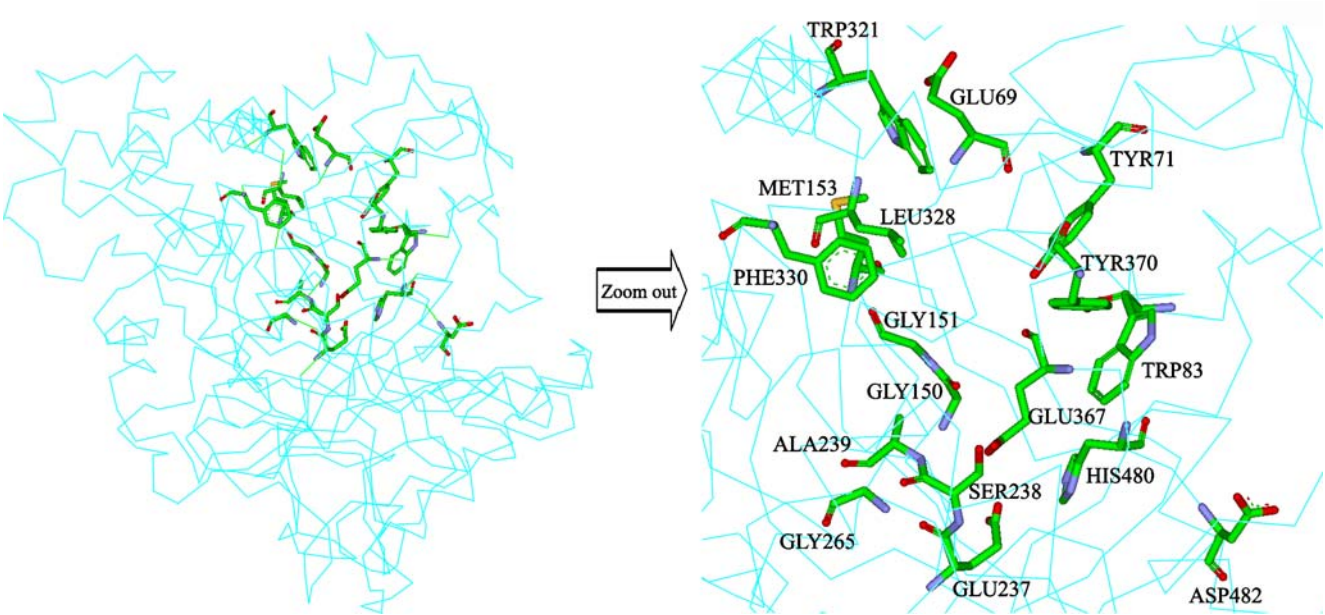

Fig. 1 Key residues (shown as sticks) in the active gorge of DmAChE (The backbone of the protein was shown as cyan.)

[34]. Each protein was minimized *in vacuo* for 10,000 steps to remove the unfavorable contacts, using the adopted basis of Newton-Raphson (ABNR) method, keeping harmonic constraints with a force constant of 20.0 kcal mol^{-1} $Å^{-1}$) on heavy atoms of the protein.

The minimized structure was then inserted into the center of a water box, keeping any atom of the protein at least 10.0 Å away from the boundary and leading to a box size of 92×91×67 $Å^3$. Water molecules closer than 1.8 Å from any atom of the protein were deleted from the water box. Seventeen sodium counterions were added at random positions into the system, at least 3.0 Å from any atom of the protein, to make the system electroneutral. The final system contained 59,868 atoms including 8812 solute atoms for Dm-S, and 57,369 atoms including 8815 solute atoms for Dm-R. The solvated system was minimized again, first with steepest descent method for 10,000 steps, then with ABNR method for 50,000 steps, to adjust the water molecules and counterions locally and eliminate any residual geometrical strain, keeping the heavy atoms of each protein fixed. The minimized solvated system served as the initial structure of the subsequent MD simulation.

Each MD simulation began with an initial and equilibration stage, followed by a 0.5-ns production run, which gave a total simulation time of 2 ns. All protein atoms were released during the process. The initial atomic velocities were assigned from a *Gaussian* distribution corresponding to a temperature of 300 K. The nonbonded energies and forces were smoothly shifted to zero at 12.0 Å [35], and a constant dielectric ($\varepsilon=1$) was used for electrostatic interactions. The nonbonded list, including neighboring atoms within a 14.0 Å distance, was updated every 20 steps. All hydrogens were treated explicitly; a time step of 2 fs was used to integrate the equations of motion with the Leapfrog Verlet algorithm. All bonds involving hydrogens were constrained with the SHAKE algorithm [36]. Coordinates and energies were saved every 500 time steps for further analysis.

In the energy minimization and the MD simulation, periodic boundary conditions were applied in all directions. The solvent and counterion images were updated every 20 steps. The NPT ensemble was implemented, using the weak coupling scheme [37] with a pressure coupling time of 5.0 ps and a temperature coupling time of 5.0 ps. The system temperature was set at 300 K, and the reference pressure of the system was set at 1.0 atm. The isothermal compressibility was set at 4.63×10–5 atm−1, and the value was approximated from experimental data for water.

After the simulation finished, an average structure was evaluated from the final 500 ps run, i.e., the whole production run. Deleting the water molecules and counterions, a 5000-step ABNR energy minimization was carried out to remove the unfavorable contacts, with 20.0 kcal mol^{-1} $Å^{-2}$ harmonic force constant on the heavy atoms. The minimized average structures were used in the analyses.

Covalent docking

17 OP and CA compounds which have different inhibitive activities to Dm-S and Dm-R were obtained from Menozzi et al. [2]. These compounds were used to assess whether the two models (i.e., Dm-S and Dm-R) could present the insecticidal resistance or not. The compounds were docked into the averaged structures of Dm-S and Dm-R after dynamics simulation by GOLD3.1 program [38]. The active site was defined as the region around the serine 238 in 10 Å. Because there would be a covalent bond between the serine 238 and insecticide molecules when the OPs and CAs inhibit the DmAChE, the covalent docking option was chosen. And the type of link was set as atom to atom. Chemscore [39, 40] in GOLD was used to score the 17 insecticides.

Results and discussion

Structural changes caused by G265A

The wild type and mutant enzymes were stable after 1500 ps simulation, as the root-mean-square deviations (RMSDs) shown in Fig. 2. The averaged structures of Dm-S and Dm-R are shown in Fig. 3 a and b, respectively. The Gly265 is positioned behind the active Ser238. Clearly, in Fig. 3 c, which displays the superposition of the mutational residues, A265 has one more methyl group than G265. The methyl group directly results in the Ser238 shift. After that, a large change of the active gorge was found.

The RMSD and RMSF values of the key residues, which are in the active gorge of DmAChE, were obtained as shown in Fig. 4 a and b. All the RMSD and RMSF values were for all atoms.

Then from Fig. 4 a and b, it can be observed that most of the key residues RMSD and RMSF values of Dm-R were lower than those of Dm-S except some residues: W83, I161, G265A and P330. After Gly265 mutated to Ala265, residues in catalytic triad (Ser238, Glu367, His480) and oxyanion hole (Gly150, Gly151, Ala239) had much lower RMSD and RMSF values than before, indicating that the active gorge of Dm-S is much more flexible than that of Dm-R. Dm-R lost the flexibility that lead to the reduction of inhibition with the insecticides. This may be one of the reasons for insecticidal resistance.

Notably, W83 and I161 of Dm-R had much higher RMSD values than those of Dm-S. The conformations of these residues changed a lot (See Fig. 5). As usual, W83 is

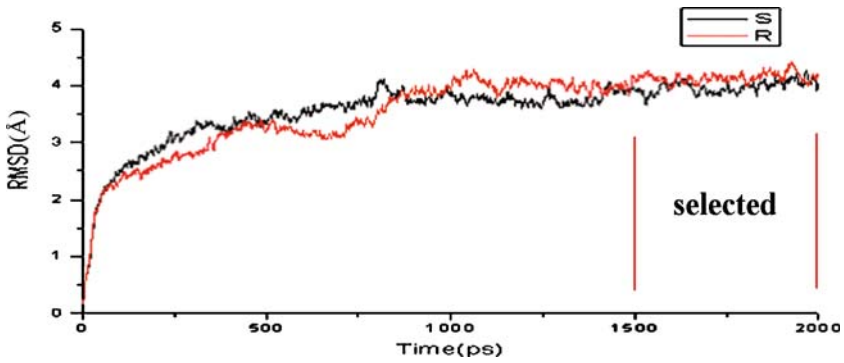

Fig. 2 RMSDs of dynamics simulation (Black for Dm-S and Red for Dm-R)

one of the residues in the "back door" for accelerating the small molecules leaving [41]. And W83 has more flexibility than other residues [42]. I161 is located at the bottom of the active site behind W83. Its side chain directly affects the freedom of W83 [4]. However, I161 located far from W83 after mutation, widening the "back door" channel to accelerate the catalysis. This may also accelerate the detoxication to insecticides.

Furthermore, A265 and F330 of Dm-R had higher RMSF values than G265 and F330 of Dm-S. A265 has one more methyl than G265 that results in higher RMSF. This mutation modified the orientation of serine 238. This changed orientation increases acetylation by the substrate as well as deacetylation, and then it induces the advance of synapse cleaning efficiency [4]. F330, as a 'swinging gate', has a wide range of conformations, which were analyzed by Kryger et al. [43]. The high RMSF value might be caused by the wide range of conformations, and the mutation let F330 get even more conformations.

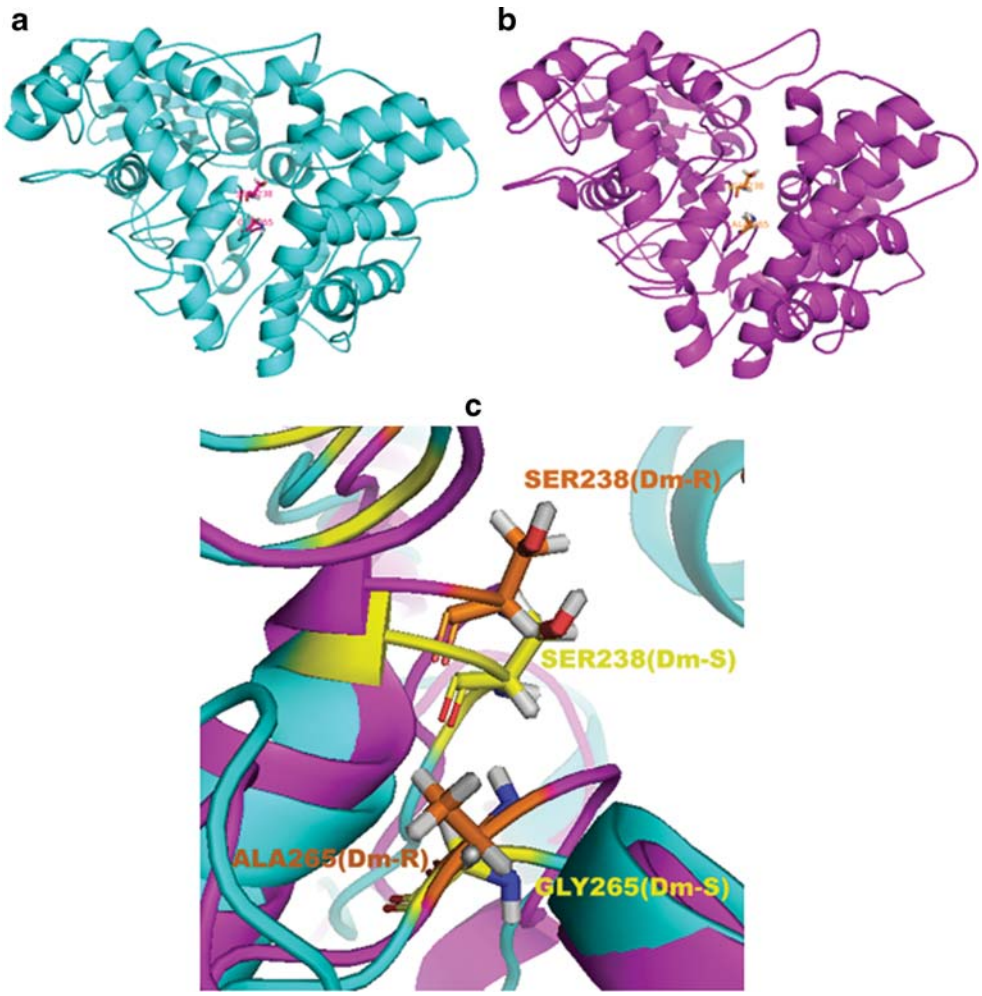

Fig. 3 **a**) Average structure of Dm-S (Red residues for G265 and S238); **b**) Average structure of Dm-R (Orange residues for A265 and S238); **c**) Close up of the superposition of the mutational residue

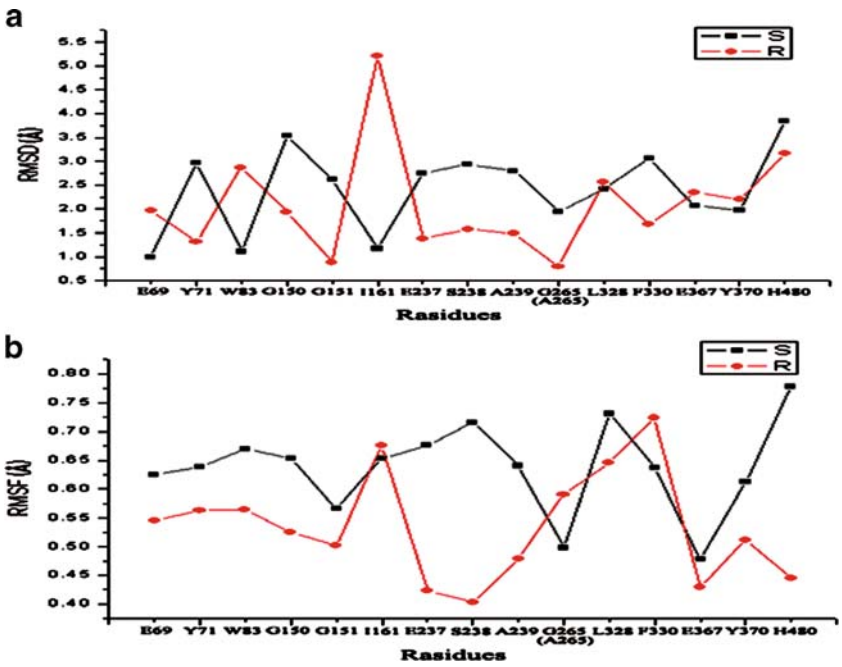

Fig. 4 **a**) RMSD values of the key residues; **b**) RMSF values of the key residues. (Black for Dm-S and Red for Dm-R) (All values based on all atoms in last 500 ps)

Some distances between S238 and other key residues around it were tracked. The distance of Tyr71 and Met153, which are the neck of active gorge mentioned by Harel et al. [23], was tracked as well. The distances changing between key residues were calculated from the whole 2 ns period. Both of Dm-S and Dm-R were calculated for comparison as shown in Fig. 6. From the last 500 ps simulation, all the distances in Dm-R became shorter than those in Dm-S. Also the average structural key residues superposition was shown in Fig. 7 which indicated the distance changing.

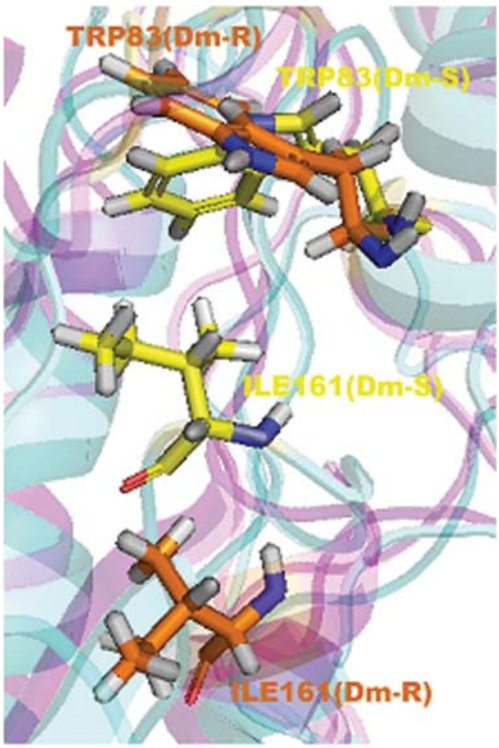

Fig. 5 The superposition of the conformations of W83 and I161 (Yellow for Dm-S and Orange for Dm-R)

From Fig. 6 a, the His480 of Dm-R was closer to the Ser238 than that of Dm-S. The last 500 ps average value of distance was 4.4 Å to 2.2 Å. Both Ser238 and His480 are directly involved in acetylate and deacetylate reactions with ACh. And the acetylate reaction is facilitated by simultaneous proton transfer from Ser238 to His480 [44]. The shorter distance between these two residues of Dm-R would shorten the distance of proton transfer so that the acetylation might be increased. Moreover, Shi et al. [4] had proved that G265A increased acetylation as well as deacetylation. Bar-On et al. [45] had reported that the inhibitor from the RIV/AChE conjugates separated the catalytic triad. So the G265A mutation would relieve this separation to reduce the inhibition.

Figure 6 b and c respectively showed the distance changing between Ser238 and Gly150 as well as between Ser238 and Gly151. The last 500 ps average value of distance was 7.4 Å (Dm-S) to 5.3 Å (Dm-R) and 8.8 Å (Dm-S) to 6.2 Å (Dm-R), respectively. Gly150 and Gly151 are parts of the oxyanion hole. These two residues always form hydrogen bonds with the carbonyl oxygen of the inhibitor that make the system stable [43]. However, after the G265A mutation, the distance between Ser238 and the oxyanion hole became small. In the same way, the space within these residues became smaller. This changing may deeply influence the binding between the insecticides and DmAChE.

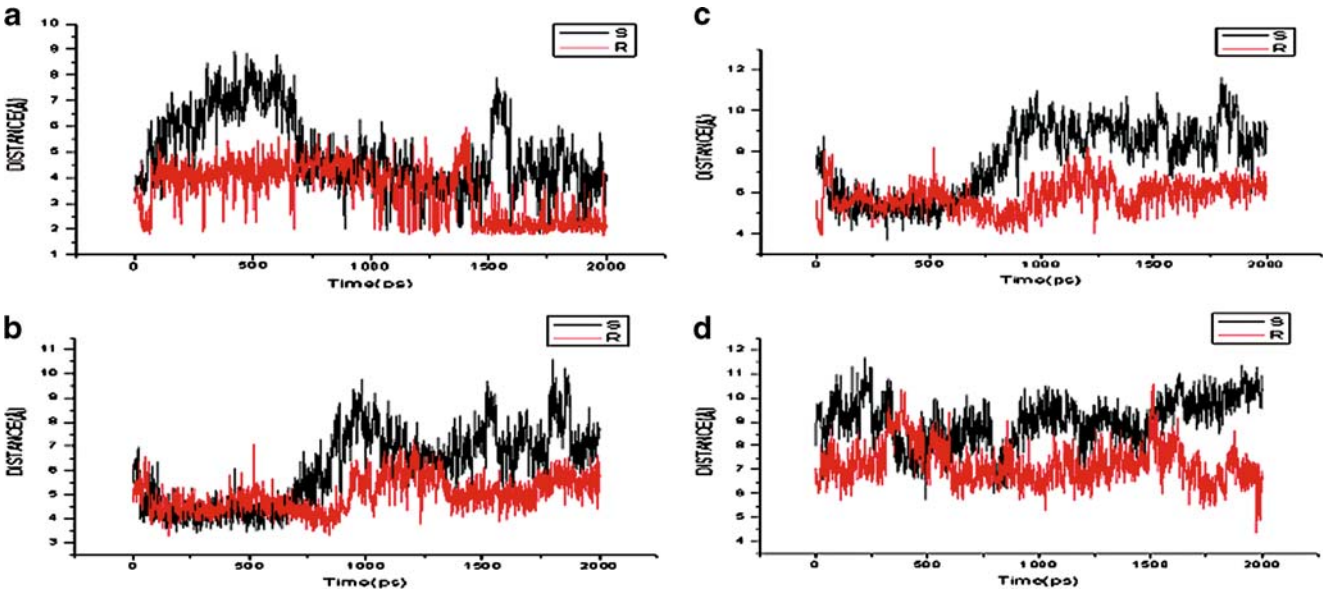

Fig. 6 **a**) The distance changing between S238(OG)-H480(NE2); **b**) The distance changing between S238(OG)-G150(HN); **c**) The distance changing between S238(OG)-G151(HN); **d**) The distance changing between Y71(OH)-M153(SD). (Black for Dm-S and Red for Dm-R)

As a whole, the shifted Ser238 lead to shorten the distances with other residues, such as Gly150, Gly151 and His480 which play important parts in the reactions with Ach. As a result, the space of the active gorge, where it could accommodate inhibitor molecules, became smaller so that it reduced the binding ability of inhibitors. Figure 7 shows that the key residues of Dm-R had a contraction relative to Dm-S.

Additionally, Tyr71 and Met153 are the neck of the active gorge so that whether an inhibitor molecule could enter into the active gorge deeply depended on the distance between these two residues [23]. The distance changing between Tyr71 and Met153 was shown in Fig. 6 d. The last 500 ps average value of distance was 9.9 Å (Dm-S) to 7.1 Å (Dm-R). The distance of Dm-R was smaller than that of Dm-S, i.e., the channel to the active site became narrower than before, so that the insecticidal resistance occurred.

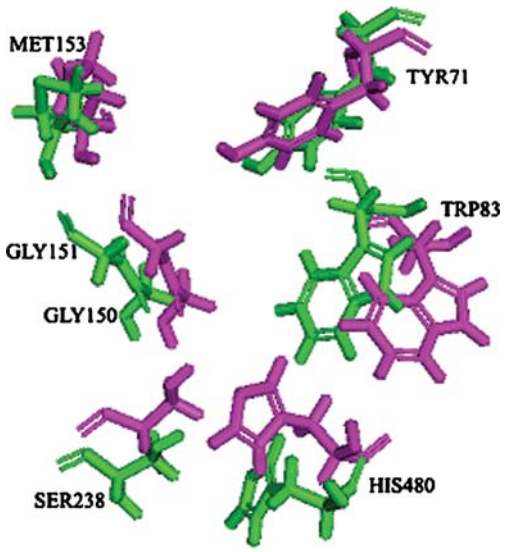

Fig. 7 Superposition of key residues in active gorge by average structures (Green for Dm-S and Magenta for Dm-R)

Table 1 17 compounds top ranked chemscores

No.	Insecticides	Group	Dm-S	Dm-R	S-R
1	methyl-azinphos	OP	17.89	−7.78	25.67
2	carbaryl	CA	27.66	−4.15	31.81
3	carbofuran	CA	26.04	−7.8	33.84
4	chlopyriphos oxon	OP	24.7	−12.88	37.58
5	coumaphos oxon	OP	13.37	−24.11	37.48
6	diazinon oxon	OP	14.11	−31.88	45.99
7	dichlorvos	OP	12.34	−10.25	22.59
8	omethoate	OP	6.77	−14.67	21.44
9	malaoxon	OP	8.59	−25.1	33.69
10	methamidophos	OP	6.21	−2.58	8.79
11	methiocarbe	CA	25.01	−4.47	29.48
12	monocrotophos	OP	8.07	−19	27.07
13	paraoxon	OP	14.06	−25.66	39.72
14	methyl-paraoxon	OP	11.88	−22.3	34.18
15	pirimicarbe	CA	21.7	−13.75	35.45
16	propoxur	CA	26.09	−7.57	33.66
17	triazophos oxon	OP	7.49	−26.66	34.15

All the insecticides were selected from ref. [2]. OP means the organophosphate and CA means the carbamate.

Different ligand docking models revealed

Seventeen OP and CA compounds were docked into Dm-S and Dm-R by GOLD3.1. The top ranked chemscore of each compound was listed in Table 1. In this part, it considered whether the covalent bonds formed by each compound were reasonable or not. After docking, the whole inhibitor of each was connected with Dm-S and Dm-R respectively, and also the leaving group, which does not take part in the covalent reaction according to the inhibition mechanism [46] was still connected with the inhibitor.

In our expectation, all of the chemscores of Dm-R were much lower than those of Dm-S. Then the extent of insecticidal resistance could be represented as Chemscore (S-R) = Chemscore(Dm-S) — Chemscore(Dm-R). Dm-S got high values of chemscores, which implied that the OPs and CAs could connect with Dm-S stably. It could change into transition state to make the leaving group leave favorably. On the contrary, Dm-R got low values of chemscores, which implied the connection between inhibitors and Dm-R was unreasonable. This also presented the resistance of Dm-R. As these docked compounds have different insecticidal resistance for alerted DmAChE assessed by Menozzi et al. [2], it verified the different insecticidal resistance presented by the models (i.e., Dm-S and Dm-R). The reliability and rationality of the models were evaluated.

Conclusions

In summary, the models of two strains of DmAChE were constructed. One was the insecticide sensitive strain (wild type): Dm-S and the other was the insecticidal resistance strain (mutational type): Dm-R which has a single point mutation (G265A). Only a conservative residue mutated caused a 'butterfly effect' that gives high insecticaidal resistance. Each model was given a total 2000 ps dynamics simulation to expose the insecticidal resistance mechanism with the comparison. The glycine 265 is highly conserved in the cholinesterase family and its mutation to alanine modified the orientation of serine 238. This mutation led to the active gorge conformation of DmAChE extremely different from the wild type. The active gorge of Dm-R was much less flexible than that of Dm-S. The "back door" channel was widened to accelerate the detoxication to insecticides by the conformation changing of W83 and I161. All the distances (S238-H480, S238-G150, S238-G151, Y71-M153) in Dm-R became smaller than those in Dm-S. These changing resulted in space reduction in the active gorge which deeply influenced the binding between the insecticides and DmAChE. Seventeen OP and CA compounds were covalent docked into Dm-S and Dm-R. The top ranked chemscores of Dm-R were much lower than those of Dm-S which exposed the insecticidal resistance for mutational DmAChE. It is believed that the present study will help to clarify the insecticidal resistance mechanism of mutational DmAChE and structure-resistance relationships, which will provide a chance for changing resistance to selectivity. And discovery of new potent insecticides to replace OPs and CAs, which has high toxicity to nature, is very urgent now.

Acknowledgments The financial supports the National Natural Science Foundation of China (grants 20802018 and 20872034), the Natural Science Foundation of Shanghai (grant 08ZR1406500), the Specialized Research fund for the Doctoral Program of Higher Education (grant 200802511002), and Shanghai Leading Academic Discipline Project (B507) are acknowledged. We would like to thank Drug Discovery and Design Center, Shanghai Institute of Materia Medica, Chinese Academy of Sciences, who provided us much help.

References

1. Matsumura F (1985) Toxicology of Insecticides, 2nd edn. Plenum, New York, p 598
2. Menozzi P, Shi M, Lougarre A, Tang Z, Fournier D (2004) Mutations of acetylcholinesterase which confer insecticidal resistance in drosophila melanogaster populations. In: BMC Evolutionary Biology, 4. Available via DIALOG. http://www.biomedcentral.com/1471-2148/4/4
3. Aldridge WN (1950) Some properties of specific cholinesterase with particular reference to the mechanism of inhibition by diethyl p-nitrophenyl thiophosphate (E605) and analogues. Biochem J 46:451–460
4. Shi M, Lougarre A, Alies C, Frémaux I, Tang Z, Stojan J, Fournier D (2004) Acetylcholinesterase alterations reveal the fitness cost of mutations conferring insecticidal resistance. In: BMC Evolutionary Biology, 4. Available via DIALOG. http://www.biomedcentral.com/1471-2148/4/5
5. Aiki Y, Kozaki T, Mizuno H, Kono Y (2005) Amino acid substitution in Ace paralogous acetylcholinesterase accompanied by organophosphate resistance in the spider mite Tetranychus kanzawai. Pestic Biochem Physiol 82:154–161
6. Hawkes NJ, Janes RW, Hemingway J, Vontas J (2005) Detection of resistance—associated point mutations of organophosphate—insensitive acetylcholinesterase in the olive fruit fly, Bactrocera oleae (Gmelin). Pestic Biochem Physiol 81:154–163
7. Andrews MC, Callaghan A, Field LM, Williamson MS, Moores GD (2004) Identification of mutations conferring insecticide—insensitive AChE in the cotton-melon aphid, Aphis gossypii glover. Insect Mol Biol 13:555–561
8. Li F, Han Z (2004) Mutations in acetylcholinesterase associated with insecticidal resistance in the cotton aphid, Aphis gossypii glover. Insect Biochem Mol Biol 34:397–405
9. Kovarik Z, Radic Z, Berman HA, Simeon-Rudolf V, Reiner E, Taylor P (2003) Acetylcholinesterase active centre and gorge conformations analysed by combinatorial mutations and enantiomeric phosphonates. Biochem J 373:33–40
10. Villatte F, Ziliani P, Marcel V, Menozzi P, Fournier D (2000) A high number of mutations in insect acetylcholinesterase may provide insecticidal resistance. Pestic Biochem Physiol 67:95–102
11. Benting J, Nauen R (2004) Biochemical evidence that an S431F mutation in acetylcholinesterase−1 of Aphis gossypii mediates

resistance to pirimicarb and omethoate. Pest Manag Sci 60:1051–1055
12. Mutero A, Pralavorio M, Bride JM, Fournier D (1994) Resistance-associated point mutations in insecticide-insensitive acetylcholinesterase. Proc Natl Acad Sci USA 91:5922–5926
13. Nabeshima T, Kozaki T, Tomita T, Kono Y (2003) An amino acid substitution on the second acetylcholinesterase in the pirimicarb—resistant strains of the peach potato aphid. Myzus persicae. Biochem Biophys Res Commun 307:15–22
14. Toda S, Komazaki S, Tomita T, Kono Y (2004) Two amino acid substitutions in acetylcholinesterase associated with pirimicarb and organophosphorous insecticidal resistance in the cotton aphid. Aphis gossypii glover (Homoptera:Aphididae). Insect Mol Biol 13:549–553
15. Fournier D, Karch F, Bride JM, Hall LMC, Bergé JB, Spierer P (1989) Drosophila melanogaster acetylcholinesterase gene structure, evolution and mutations. J Mol Biol 210:15–22
16. Weill M, Malcolm C, Chandre F, Mogensen K, Berthomieu A, Marquine M, Raymond M (2004) The unique mutation in ace−1 giving high insecticidal resistance is easily detectable in mosquito vectors. Insect Mol Biol 13:1–7
17. Weill M, Fort P, Berthomieu A, Dubois MP, Pasteur N, Raymond M (2002) A novel acetylcholinesterase gene in mosquitoes codes for the insecticide target and is non-homologous to the ace gene in Drosophila. Proc R Soc London, Ser B 269:2007–2016
18. Baek JH, Kim JI, Lee DW, Chung BK, Miyata T, Lee SH (2005) Identification and characterization of ace1-type acetylcholinesterase likely associated with organophosphate resistance in plutella xylostella. Pestic Biochem Physiol 81:164–175
19. Hall LMC, Spierer P (1986) The ace locus of drosophila melanogaster: structural gene for acetylcholinesterase with an unusual 5' leader. EMBO J 5:2949–2954
20. Guedes RNC, Zhu KY, Kambhampati S, Dover BA (1997) An altered acetylcholinesterase conferring negative cross—insensitivity to different insecticidal inhibitors in organophosphate—resistant lesser grain borer, rhyzopertha dominica. Pestic Biochem Physiol 58:55–62
21. Villatte F, Augé D, Touton P, Delorme R, Fournier D (1999) Negative cross-insensitivity in insecticide—resistant cotton aphid aphis gossypii glover. Pestic Biochem Physiol 65:55–61
22. Brown AWA (1961) Negatively-correlated insecticides: a possible countermeasure for insecticidal resistance. Pest Control 29:24–26
23. Harel M, Kryger G, Rosenberry TL, Mallender WD, Lewis T, Fletcher RJ, Guss JM, Silman I, Sussman JL (2000) Three-dimensional structures of drosophila melanogaster acetylcholinestase and of its complexes with two potent inhibitors. Protein Sci 9:1063–1072
24. Millard CB, Kryger G, Ordentlich A, Greenblatt HM, Harel M, Raves ML, Segall Y, Barak D, Shafferman A, Silman I, Sussman JL (1999) Crystal structures of aged phosphonylated acetylcholinesterase: nerve agent reaction products at the atomic level. Biochemistry 38:7032–7039
25. Tang Y, Nilsson L (1998) Interaction of human SRY protein with DNA: A molecular dynamics study. PROTEINS: Structure, Function, and Genetics 31:417–433
26. Xu Y, Barrantes FJ, Luo X, Chen KX, Shen JH, Jiang H (2005) Conformational dynamics of the nicotinic acetylcholine receptor channel: a 35-ns molecular dynamics simulation study. J Am Chem Soc 127:1291–1299
27. Zhang J, Xu Y, Shen J, Luo X, Cheng J, Chen K, Zhu W, Jiang H (2005) Dynamic Mechanism for the Autophosphorylation of CheA Histidine Kinase: Molecular Dynamics Simulations. J Am Chem Soc 127:11709–11719
28. Kong Y, Ma J (2001) Dynamic Mechanisms of the Membrane Water Channel Aquaporin−1 (AQP-1). Proc Natl Acad Sci 98:14345–14349
29. Alonso H, Bliznyuk AA, Gready JE (2006) Combining docking and molecular dynamics simulations in drug design. Med Res Rev 26:531–568
30. Brooks BR, Bruccoleri RE, Olafson BD, States DJ, Swaminathan S, Karplus M (1983) CHARMM: a program for macromolecular energy, minimization, and dynamics calculations. J Comput Chem 4:187–217
31. MacKerell AD Jr, Bashford D, Bellott M, Dunbrack RL Jr, Evanseck JD, Field MJ, Fischer S, Gao J, Guo H, Ha S, Joseph-McCarthy D, Kuchnir L, Kuczera K, Lau FTK, Mattos C, Michnick S, Ngo T, Nguyen DT, Prodhom B, Reiher WE III, Roux B, Schlenkrich M, Smith JC, Stote R, Straub J, Watanabe M, Wiorkiewicz-Kuczera J, Yin D, Karplus M (1998) All-atom empirical potential for molecular modeling and dynamics studies of proteins. J Phys Chem B 102:3586–3616
32. MacKerell AD Jr, Wiorkiewicz-Kuczera J, Karplus M (1995) An all-atom empirical energy function for the simulation of nucleic acids. J Am Chem Soc 117:11946–11975
33. Jorgensen WL, Chandrasekhar J, Madura JD, Impey RW, Klein ML (1983) Comparison of simple potential functions for simulating liquid water. J Chem Phys 79:926–935
34. Brünger A, Karplus M (1988) Polar hydrogen positions in proteins: empirical energy placement and neutron diffraction comparison. Proteins 4:148–156
35. Steinbach PJ, Brooks BR (1994) New spherical-cutoff methods for long-range forces in macromolecular simulation. J Comput Chem 15:667–683
36. Ryckaert JP, Ciccotti G, Berendsen HJC (1977) Numerical integration of the cartesian equations of motion of a system with constraints: molecular dynamics of n-alkanes. J Comp Phys 23:327–341
37. Berendsen HJC, Postma JPM, van Gunsteren WF, DiNola A, Haak JR (1984) Molecular dynamics with coupling to an external bath. J Chem Phys 81:3684–3690
38. Jones G, Willet P, Glen RC, Leach AR, Taylor RJ (1997) Development and validation of a genetic algorithm for flexible docking. J Mol Biol 267:727–748
39. Eldridge MD, Murray CW, Auton TR, Paolini GV, Mee RP (1997) Empirical scoring functions: I. The development of a fast empirical scoring function to estimate the binding affinity of ligands in receptor complexes. J Comput-Aided Mol Des 11:425–445
40. Baxter CA, Murray CW, Clark DE, Westhead DR, Eldridge MD (1998) Flexible docking using tabu search and an empirical estimate of binding affinity. Proteins 33:367–382
41. Gilson MK, Straatsma TP, McCammon JA, Ripoll DR, Faerman CH, Axelsen PH, Silman I, Sussman JL (1994) Open 'back door' in a molecular dynamics simulation of acetylcholinesterase. Science 263:1276–1278
42. Simon S, Le Goff A, Frobert Y, Grassi J, Massoulie J (1999) The binding sites of inhibitory monoclonal antibodies on acetylcholinesterase. Identification of a novel regulatory site at the putative "back door". J Biol Chem 274:27740–27746
43. Kryger G, Silman I, Sussman JL (1999) Structure of acetylcholinesterase complexed with E2020(Aricept): implications for the design of new anti-Alzheimer drugs. Structure 7:297–307
44. Zhang Y, Kua J, McCammon JA (2002) Role of the catalytic triad and oxyanion hole in acetylcholinesterase catalysis: an ab initio QM/MM study. J Am Chem Soc 124:10572–10577
45. Bar-On P, Millard CB, Harel M, Dvir H, Enz A, Sussman JL, Silman I (2002) Kinetic and structural studies on the interaction of cholinesterases with the anti-alzheimer drug rivastigmine. Biochemistry 41:3555–3564
46. Aldridge WN (1950) Some properties of specific cholinesterase with particular reference to the mechanism of inhibition by diethyl p-nitrophenyl thiophosphate (E605) analogues. Biochem J 46:451–460